ESTIMATE OF THE LARGEST LYAPUNOV CHARACTERISTIC EXPONENT OF A HIGH DIMENSIONAL ATMOSPHERIC GLOBAL CIRCULATION MODEL

A sensitivity analysis

ALESSANDRO GUERRIERI

ENEA - Clima Globale - Unità Simulazioni Atmosferiche
Centro Ricerche Casaccia, Roma

RT/2009/21/ENEA

AGENZIA PER LE NUOVE TECNOLOGIE,
L'ENERGIA E LO SVILUPPO ECONOMICO SOSTENIBILE

ESTIMATE OF THE LARGEST LYAPUNOV CHARACTERISTIC EXPONENT OF A HIGH DIMENSIONAL ATMOSPHERIC GLOBAL CIRCULATION MODEL

A sensitivity analysis

ALESSANDRO GUERRIERI

ENEA - Clima Globale - Unità Simulazioni Atmosferiche
Centro Ricerche Casaccia, Roma

RT/2009/21/ENEA

ESTIMATE OF THE LARGEST LYAPUNOV CHARACTERISTIC EXPONENT OF A HIGH DIMENSIONAL ATMOSPHERIC GLOBAL CIRCULATION MODEL

A sensitivity analysis

ALESSANDRO GUERRIERI

Abstract
In this report the largest Lyapunov characteristic exponent of a high dimensional atmospheric global circulation model of intermediate complexity has been estimated numerically. A sensitivity analysis has been carried out by varying the equator-to-pole temperature difference, the space resolution and the value of some parameters employed by the model. Chaotic and non-chaotic regimes of circulation have been found.

Key words: *atmospheric general circulation, high dimensional chaos, Lyapunov characteristic exponent, modelling and model calibration, nonlinear dynamical systems*

Riassunto
In questo rapporto il massimo esponente caratteristico di Lyapunov di un modello di circolazione atmosferica globale a complessità intermedia è stato stimato numericamente. E' stata condotta un analisi di sensibilità in funzione della differenza di temperatura equatore-polo, della risoluzione spaziale e di alcuni parametri impiegati dal modello. Sono stati individuati regimi di circolazione caotici e non caotici.

Parole chiave: circolazione generale dell'atmosfera, caos a dimensionalità elevata, esponente caratteristico di Lyapunov, modellistica e calibrazione dei modelli, sistemi dinamici non lineari

Contents

1 Introduction

It is well known that chaotic nonlinear dynamical systems are characterized by a strong sensitivity to initial conditions: two trajectories (in the phase space) of a dynamical system separated by a tiny initial distance will depart exponentially, making it impossible to predict the future state of the system because of the inevitable inaccuracy and incompleteness with which its initial conditions are known [1, 2]. This aspect is particularly relevant for the evolution of the atmospheric circulation when it is analyzed in view of its use for wheather forecasts and climate modelling [3]. In general, a positive Lyapunov Characteristic Exponent (LCE) is the signature of chaos in dynamical systems. The present work has been stimulated by the results obtained by Lunkeit [4], where the largest LCE was estimated (albeit hard to be validated, as it was observed by its author) by synchronizing two identical high dimensional atmospheric global circulation models exhibiting chaotic behaviors. Here, our aim is to analyse the sensitivity of the largest LCE on equator-to-pole temperature differences, spatial resolutions and some parameters employed by the same atmospheric global circulation model used by [4]. To this purpose we follow the procedure proposed by Benettin *et al.* [5] to find out the numerical value of the largest LCE. Chaotic and non-chaotic regimes of the model have been found by varying the equator-to-pole temperature difference.

This paper is organized as follows: the atmospheric model is described briefly in Sec. II; the methodology employed to find the largest LCE is described in Sec. III; Section IV reports the experimental set-up and the results obtained; finally, in Sec. V a discussion of the results is presented together with some concluding remarks.

2 Model

We are interested into the estimate of the largest LCE of a high dimensional atmospheric global circulation model of intermediate complexity named PUMA. This model, described in [6, 7], is based on the numerical solution of a set of equations modelling the fluid motion of a dry atmosphere in spherical geometry. Here, for the sake of completeness, the equations of the PUMA model are reported:

$$\frac{\partial \zeta}{\partial t} - \frac{1}{1-\mu^2}\frac{\partial \mathcal{F}_v}{\partial \lambda} + \frac{\partial \mathcal{F}_u}{\partial \mu} = -\frac{\xi}{\tau_f} - K(-1)^h \nabla^{2h} \xi, \tag{1}$$

$$\frac{\partial D}{\partial t} - \frac{1}{1-\mu^2}\frac{\partial \mathcal{F}_u}{\partial \lambda} - \frac{\partial \mathcal{F}_v}{\partial \mu} = -\nabla^2 \left(\frac{U^2+V^2}{2(1-\mu^2)} + \Phi + \overline{T} \ln p_s \right) - \frac{D}{\tau_f} - K(-1)^h \nabla^{2h} D, \tag{2}$$

$$\frac{\partial T'}{\partial t} + \frac{1}{1-\mu^2}\frac{\partial (UT')}{\partial \lambda} + \frac{\partial (VT')}{\partial \mu} = DT' - \dot{\sigma}\frac{\partial T}{\partial \sigma} + \kappa \frac{T\omega}{p} + \frac{T_R - T}{\tau_c} - K(-1)^h \nabla^{2h} T', \tag{3}$$

$$\frac{\partial (\ln p_s)}{\partial t} + \frac{U}{1-\mu^2}\frac{\partial (\ln p_s)}{\partial \lambda} + V\frac{\partial (\ln p_s)}{\partial \mu} = -D - \frac{\partial \dot{\sigma}}{\partial \sigma}, \tag{4}$$

$$\frac{\partial \Phi}{\partial \ln \sigma} = -T, \tag{5}$$

with

$$\mathcal{F}_u = V\zeta - \dot{\sigma}\frac{\partial U}{\partial \sigma} - T'\frac{\partial (\ln p_s)}{\partial \lambda}$$

and

$$\mathcal{F}_v = -U\zeta - \dot{\sigma}\frac{\partial V}{\partial \sigma} - T'(1-\mu^2)\frac{\partial (\ln p_s)}{\partial \mu}.$$

Absolute and relative vorticity are represented by ζ and ξ, respectively. D is the horizontal divergence. The temperature $T = \overline{T} + T'$ is expressed by the sum of the constant reference temperature $\overline{T}$ and an anomaly T'. Longitude and latitude are expressed by λ and ϕ, respectively, with $\mu = \sin\phi$. The

vertical coordinate is $\sigma = p/p_s$, where p and p_s indicate pressure and surface pressure, respectively. Φ is the geopotential, κ is the adiabatic coefficient (i.e.: $\kappa = R/c_p$, where R is the gas constant for dry air, and c_p is the specific heat capacity for dry air at constant pressure). The vertical velocity is ω, $U = u\cos\phi$ and $V = v\cos\phi$ where u and v are the zonal and meridional components of the horizontal velocity, respectively. Three parameterizations are employed: hyperdiffusion, Rayleigh friction and Newtonian cooling. Hyperdiffusion, proportional to ∇^{2h} by means of the coefficient K, is applied to temperature, divergence and vorticity for the subgrid scaling of eddies: it is assumed to be acting on all waves with a time scale damping equal to 0.25 day on the smallest resolved wave; h is an integer equal to 4 for all simulations. Rayleigh friction acts on divergence and vorticity to model large scale dissipation: it is assumed to be confined to the lowermost level with a time scale τ_f of 1 day. Newtonian cooling parameterizes the driving term: it represents diabatic heating. The temperature relaxes toward a prescribed reference temperature T_R with a time scale τ_c equal to 30 days for all levels. Spherical harmonics transform method is used with triangular truncations T21 and T42 for the horizontal resolution and five vertical equally spaced σ levels. The model solves the prognostic equations (1-4) in terms of the spectral coefficients of vorticity, divergence, temperature and logarithm of the ground pressure, while the diagnostic equation (5) expresses the hydrostatic equilibrium.

3 Largest Lyapunov Characteristic Exponent

The methodology, proposed by [5] to calculate the largest LCE, will be described here briefly. Preliminarly, it is observed that the dynamical variables

of the atmospheric model (i.e.: vorticity, divergence, temperature and surface pressure) constitute a discrete-time dynamical system whose dimension is equal to their overall number (e.g.: 8096 for a T21 triangular truncation). The time sequence of phase-space points occupied by the dynamical system represents a trajectory. Basically, in order to find the largest LCE, we follow the time evolution of a reference trajectory and a perturbed one, initially separated by a small distance. As the time evolution of both trajectories goes on, the perturbed trajectory is kept very close to the reference one by means of a periodic rescaling applied to its variables. Let us define the following quantity:

$$k_n(\tau, \mathbf{x}_0, d_0) = \frac{1}{n\tau} \sum_{i=1}^{n} ln \left(\frac{d_i}{d_0} \right), \tag{6}$$

where $\mathbf{x}_0$ is the initial point (initial conditions) of the reference trajectory; d_0 is the euclidean initial separation of the perturbed trajectory from the reference one; d_i is the euclidean separation of the perturbed trajectory at the end of the i-th time interval of duration τ; n represents the overall number of time intervals. The separation d_i of the perturbed trajectory from the reference one is calculated as follows:

$$d_i = \|\mathbf{x}_i{}' - \mathbf{x}_i\|, \tag{7}$$

where $\mathbf{x}_i{}'$ and $\mathbf{x}_i$ are the vectors representing the dynamical variables along the perturbed trajectory and the reference one at the end of the i-th time interval. By letting rf_i be a rescaling factor defined as:

$$rf_i = \frac{d_0}{d_i}, \tag{8}$$

the dynamical variables $\mathbf{x}_i{}'$ of the perturbed trajectory are rescaled as follows:

$$\widehat{\mathbf{x}}_i = \mathbf{x}_i + (\mathbf{x}_i{}' - \mathbf{x}_i)\, rf_i, \tag{9}$$

where $\widehat{\mathbf{x}}_i$ refer to rescaled quantities. According to [5], the following property holds, provided that τ and d_0 are sufficiently small:

$$\lim_{n\to\infty} k_n(\tau, \mathbf{x}_0, d_0) = \lambda_{max}, \tag{10}$$

where λ_{max} represents the largest LCE. In order to find numerically the largest LCE, the procedure described by Eqs. (7), (8) and (9) is applied n times and, if n is large enough, λ_{max} is calculated by means of Eqs. (6) and (10).

4 Experimental Set-up and Results

In order to calculate the largest LCE, λ_{max}, with the procedure previously illustrated, we need to generate a reference trajectory and a perturbed one. In all numerical experiments the model starts from rest with a small random perturbation been added to the ground pressure, and is integrated for 10 years (spin-up of the model) to reach a final state whose internal variability is well established and the memory of the initial conditions is completely lost. This final state is used as initial conditions for the reference trajectory, while the perturbed trajectory is generated by adding a small random quantity to the ground pressure that was obtained as final state at the end of the first 10 years. Both the reference trajectory and the perturbed one are 80 years long and the amplitude d_0 of their initial separation ranges from 10^{-7} to 10^{-2} (in adimensional units). A time step of 0.5 hour is adopted for the time integration of the prognostic Eqs. (1-4). The overall number n of time intervals of duration τ is about 9000. Relaxation temperature T_R [see Eq. (3)] is assumed to be zonally symmetric. Numerical computations have been performed on a IBM sp5 computer with a precision of 18 digits. A typical behaviour of k_n, as a function of $n\tau$ [see Eq. (6)], is shown in Fig. 1

where it can be seen that k_n reaches its asymptotic value λ_{max} after 10^4 days (about 30 years). The values of λ_{max} turned out to be independent of both the initial separation amplitude d_0 and the initial condition $\mathbf{x}_0$. The main results concerning the largest LCE are reported in what follows.

1. The largest LCE depends on the driving term (Newtonian cooling) expressed by the amplitude ΔT_{E-P} of the relaxation temperature difference between the equator and the poles (symmetric with respect to the equator, corresponding to equinox conditions). Sensitivity studies have been carried out for $\Delta T_{E-P} = 60 \pm 40$ K. Figures 2, 3 and 4 summarize the values of the largest LCE obtained for perturbed trajectories with initial separation d_0 from the reference ones approximately equal to 10^{-7}, 10^{-5} and 10^{-2}, respectively. From Figs. (2-4) it appears that the behaviour of the largest LCE with ΔT_{E-P} is virtually independent of the initial amplitude d_0. For T21, $\Delta T_{E-P} = 30$ K is the threshold value above which the values of the largest LCE become positive. Figures 5 and 6 show the power spectra of the global mean relative vorticity for the cases with $\Delta T_{E-P} = 80$ K and $\Delta T_{E-P} = 20$ K, respectively. Figures 7 and 8 show the autocorrelations of the global mean relative vorticity.

2. The largest LCE depends on the horizontal resolution, as it can be seen from Fig. 9 where the values of λ_{max} have been reported for T21 and T42 horizontal resolutions. Such a dependence is due to the hyperdiffusion coefficient K which is proportional to the following factor

$$\frac{1}{\tau_{diss}\left[N_{tru}\left(N_{tru}+1\right)\right]^h}, \tag{11}$$

where τ_{diss} is the dissipation time constant, N_{tru} is the truncation number of the spectral representation and h is half the order of the hy-

perdiffusion operator ∇^{2h} appearing in Eqs. (1-3). From (11) it is evident that by increasing the truncation number N_{tru} and keeping τ_{diss} unchanged, the hyperdiffusion coefficient K diminuishes and the exponential decay of the modes is slower. In this way the faster time evolution of the modes reflects itself into values of the largest LCE that are higher for T42 than for T21. The value chosen for τ_{diss} is the same as that one employed by [4] ($\tau_{diss} = 0.25$ day), for both T21 and T42 resolutions. Here it is worth noting that, in general, the order $2h$ of the hyperdiffusion operator can assume values other than that been chosen for the cases studied in this work, but it has been set equal to 8 to be consistent with [4].

3. Sensitivity studies, summarized by Figures 10 and 11, show that the largest LCE is weakly dependent on the Newtonian cooling time scale τ_c within a range of 10% of the reference value with $\tau_c = 30$ days after 80 years of simulation. This result holds both for the T21 resolution and for the T42 one. For fixed ΔT_{E-P}, the largest LCE are higher for shorter values of the cooling time constant τ_c: this last property appears to hold as long as ΔT_{E-P} is above its threshold value for chaotic regime (see Sec. V).

5 Discussion and Concluding Remarks

From Fig. 9 it appears that positive values of the largest LCE are obtained for $\Delta T_{E-P} > 30$ K (for T21) and for $\Delta T_{E-P} > 15$ K (for T42). These results imply that the atmospheric circulation becomes ordered (i.e. not chaotic) below those thresholds, although the value of the thresholds is not the same for both of the horizontal resolutions. It is worth noting that the

graphs of the largest LCE [Figs.(2-4,9)] are similar to the one reproduced in Fig. 12, taken from [5] and referring to the Hénon-Heiles model, where the largest LCE's have been indicated (with asterisks) vs. the parameter E (energy). However, unlike the Hénon-Heiles model (for $E \geq 0.1$), in our atmospheric model there seems to be no initial conditions such that, for a given ΔT_{E-P} greater than the above mentioned thresholds, we get ordered (vanishing largest LCE) and chaotic (positive largest LCE) regimes of circulation. For T21 and $\Delta T_{E-P} = 80$ K, the spectrum (Fig. 5) of the global mean relative vorticity is noisy and flattened up to time scales equal to about 100 days and its autocorrelation function (Fig. 7) is strongly decaying with time. On the contrary, for $\Delta T_{E-P} = 20$ K the power spectrum (Fig. 6) and its autocorrelation function (Fig. 8) show no characteristic sign of chaotic regimes. For T42 a similar observation applies to the power spectrum of the global mean relative vorticity and to its autocorrelation, [Figs.(13-16)]. Figures 17 and 18 show the meridional cross sections of the time average (over 80 years) of the average zonal wind for the horizontal resolutions T21 and T42, respectively, both ones with $\Delta T_{E-P} = 80$ K: position and intensity of the tropical easterlies and the westerly jets are well reproduced and consistent with the observed zonally averaged circulation. Analogously, Figs. 19 and 20 show the meridional cross sections of the time average of the average zonal wind for the horizontal resolutions T21 ($\Delta T_{E-P} = 20$ K) and T42 ($\Delta T_{E-P} = 10$ K), respectively: both zonal flows appear to be substantially stratified without the presence of the tropical easterlies.

In this paper we have used the procedure proposed by [5] to examine the sensitivity of the largest LCE of a high dimensional atmospheric global circulation model of intermediate complexity on some parameters commonly employed to describe the general atmospheric circulation, such as the equator-to-pole

temperature difference and the Newtonian cooling time scale. A direct comparison of our results with those obtained by [4] with the same set of parameters shows that the value of the largest LCE (0.08/day, see [4]), for the case with a T21 horizontal resolution and $\Delta T_{E-P} = 80$ K, is close to the one obtained here (0.074/day). However, the method proposed by [5] to find out the numerical value of the largest LCE turned out to be more straigthforward and numerically accurate than the one used by [4] which requires to look for the minimum value of the coupling strength giving complete synchronization of the two models in order to estimate the largest LCE. Furthermore, it has been shown here that the largest LCE is dependent on the horizontal resolution. In addition it has been found that the threshold value of ΔT_{E-P} marking the transition to chaotic regimes appears to depend on the space resolution itself. As a consequence of this result, one single choice of space resolution is not sufficient to establish the (chaotic/ordered) nature of atmospheric circulation regimes. Finally, a weak dependence of the largest LCE on the Newtonian cooling time scale has been found, in agreement with the conclusions of [4].

6 Acknowledgments

The author wishes to thank Prof. A. Vulpiani for useful discussions and suggestions.

7 Appendix: changes applied to PUMA

In order to carry out the numerical computations of the largest LCE, a couple of new Fortran90 modules have been introduced together with some minor

modifications to the orginal code. The whole computation can be described as a four-steps procedure:

1. For a given choice of parameters and spatial resolutions, the initial run (spin-up) is prepared starting from a fluid at rest and perturbing (the logarithm of) the ground pressure by adding a small random quantity to it. Each initial run is carried out for 10 years.

2. The final state reached at the end of step 1 is used as initial condition (i.e. $\mathbf{x}_0$, see Sec. III) to restart the model. At regular time intervals of duration τ, the prognostic variables are written on an auxiliary file by means of the new routine 'runsp' added to PUMA. This generates the reference simulation (i.e. $\mathbf{x}_i$).

3. The same final state reached at the end of step 1 is perturbed with the addition of a small random quantity to the (logarithm of the) ground pressure. This task is accomplished with a stand-alone program called 'prepdata.f90', not included in PUMA. This new state is used as the starting point of the perturbed simulation, separated from the reference one by the distance d_0. At the same time intervals of step 2, the perturbed simulation (i.e. $\mathbf{x}_i'$) is stopped, its distance d_i from the reference one is measured and the prognostic variables are rescaled according to Eq. (9). After every rescaling, the perturbed simulation is restarted and left been running for another interval at the end of which the rescaling is repeated, and so on until the end of the simulation. The whole procedure of rescaling is carried out inside the new routine 'rinorm' added to PUMA.

4. The estimate of the largest LCE, according to the procedure illustrated in Sect. III, is done as a post-processing of the data written during

the step 3 on a *ad hoc* file, where the distances d_0 and d_i have been previously recorded by the routine 'rinorm'.

References

[1] Ott, E., *Chaos in Dynamical Systems*, 2nd edition (Cambridge University Press, Cambridge, 2002).

[2] Eckmann, J.-P. and Ruelle, D., "Ergodic theory of chaos and strange attractors," Rev. Mod. Phys. **57**, 617-656, 1985.

[3] Lorenz, E. N., "Deterministic Nonperiodic Flow," J. Atmos. Sci. **20**, 130-141, 1963.

[4] Lunkeit, F, "Synchronization experiments with an atmospheric global circulation model," Chaos **11**, 47-51, 2001.

[5] Benettin, G., Galgani, L., and Strelcyn, J. M., "Kolmogorov entropy and numerical experiments," Phys. Rev. A **14**, 2338-2345, 1976.

[6] Fraedrich, K., Kirk, E., and Lunkeit, F., "PUMA: Portable University Model of the Atmosphere," Deutsches Klimarechenzentrum Technical Report No. 16, 1998.

[7] Fraedrich, K., Kirk, E., Luksch, U., and Lunkeit, F., "The portable university model of the atmosphere (PUMA): Storm track dynamics and low-frequency variability," Meteorol. Zeitschrift **14**, 735-745, 2005.

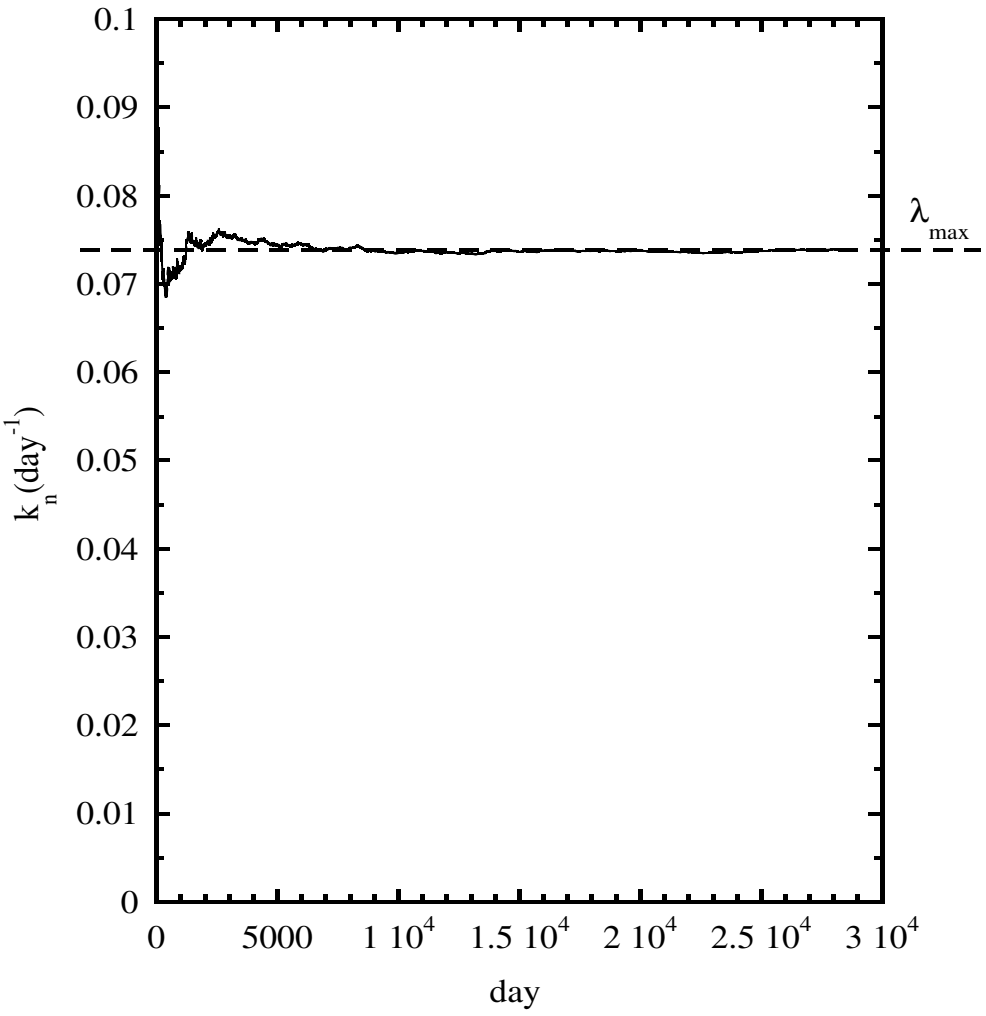

Figure 1: k_n vs. time for $\Delta T_{E-P} = 80$ K, T21 and $\tau_c = 30$ days. The asymptotic value λ_{max} reached by k_n is the largest Lyapunov characteristic exponent (see the text for further details).

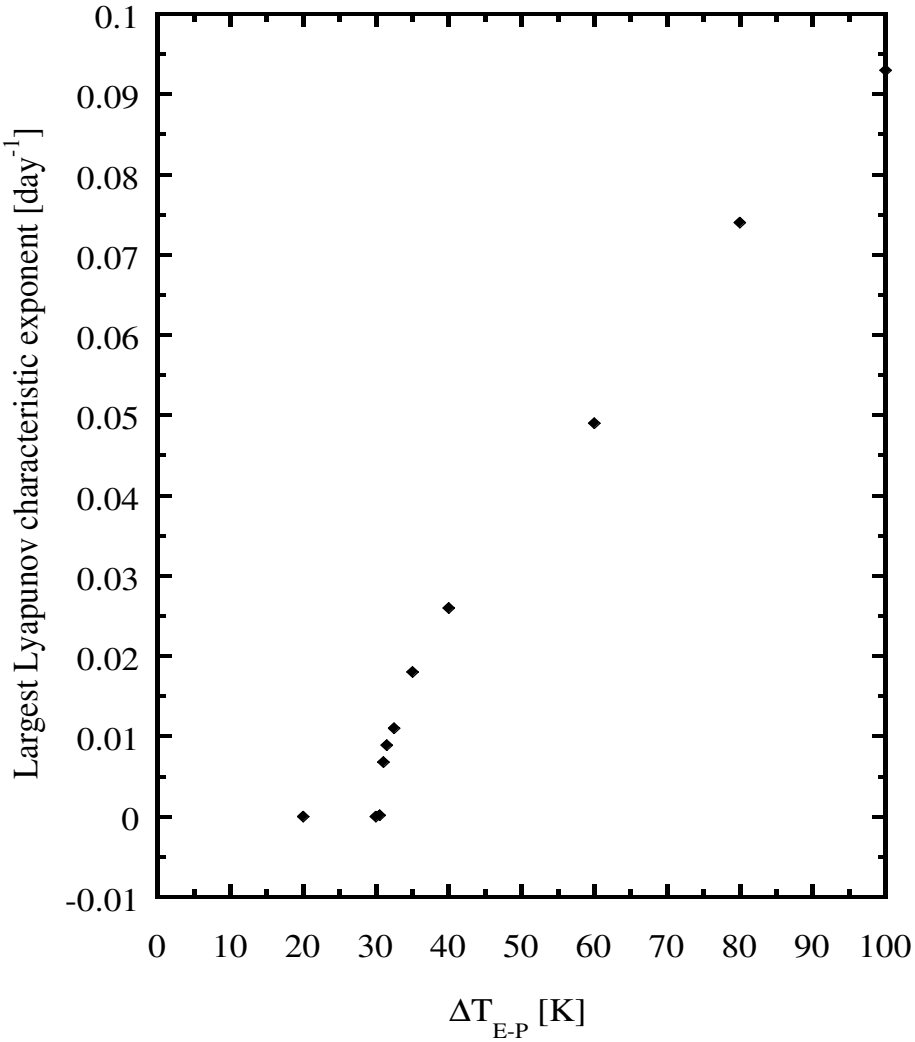

Figure 2: largest LCE vs. ΔT_{E-P}; amplitude of initial perturbation $\approx 10^{-7}$, T21 and $\tau_c = 30$ days. Nonvanishing values of the largest LCE indicate chaotic regimes of the model.

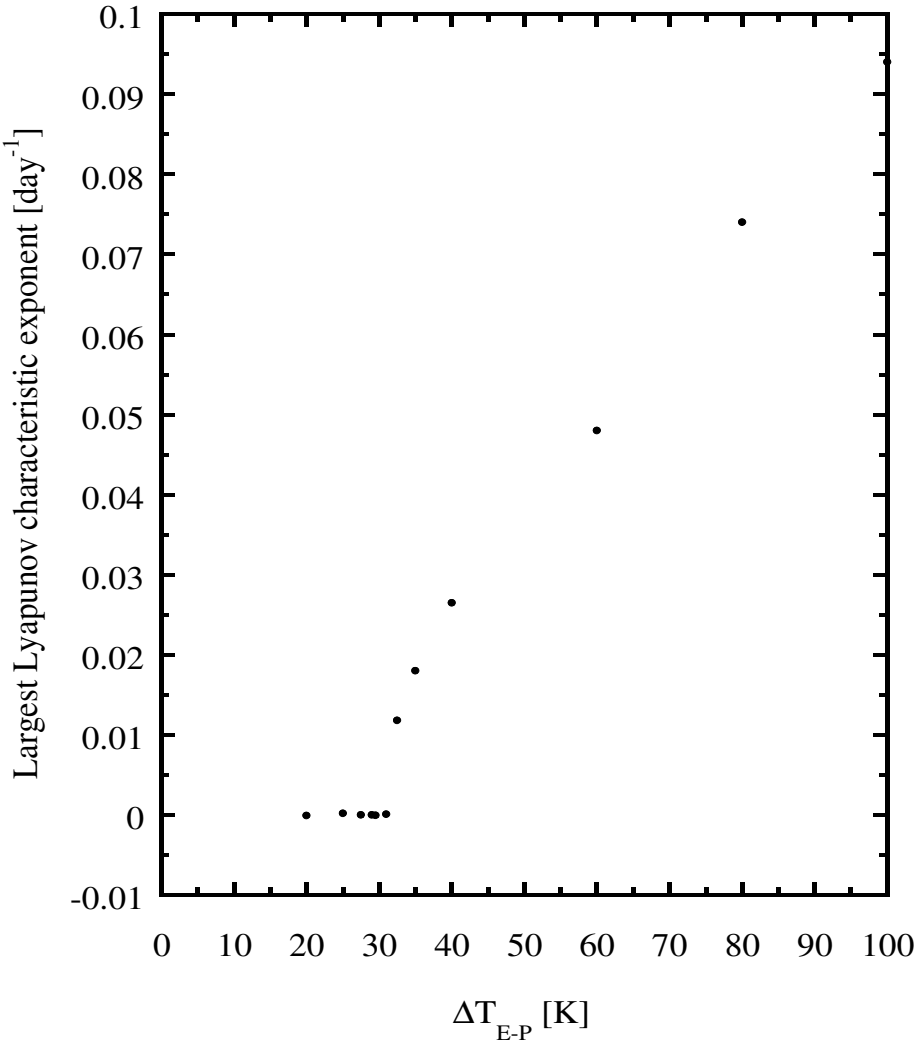

Figure 3: same as Fig. 2 (largest LCE vs. ΔT_{E-P}), but with amplitude of initial perturbation $\approx 10^{-4}$.

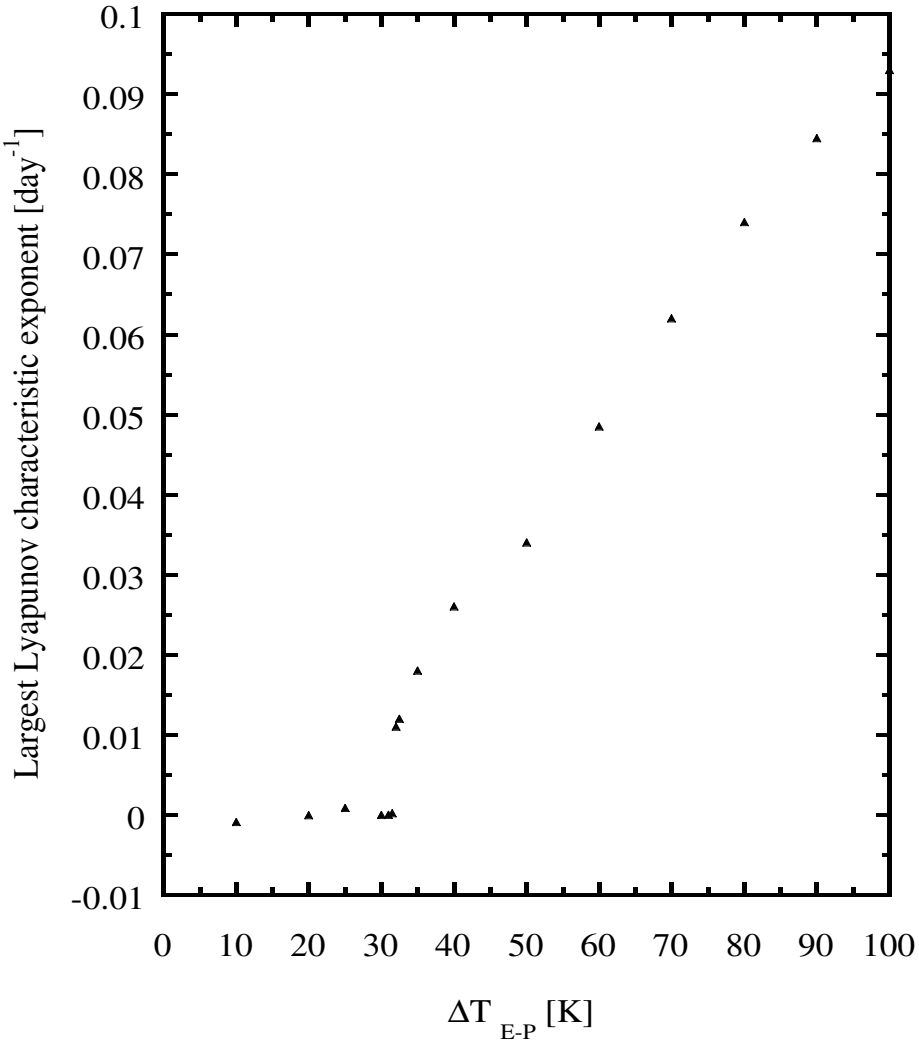

Figure 4: same as Fig. 2 (largest LCE vs. ΔT_{E-P}), but with amplitude of initial perturbation $\approx 10^{-2}$.

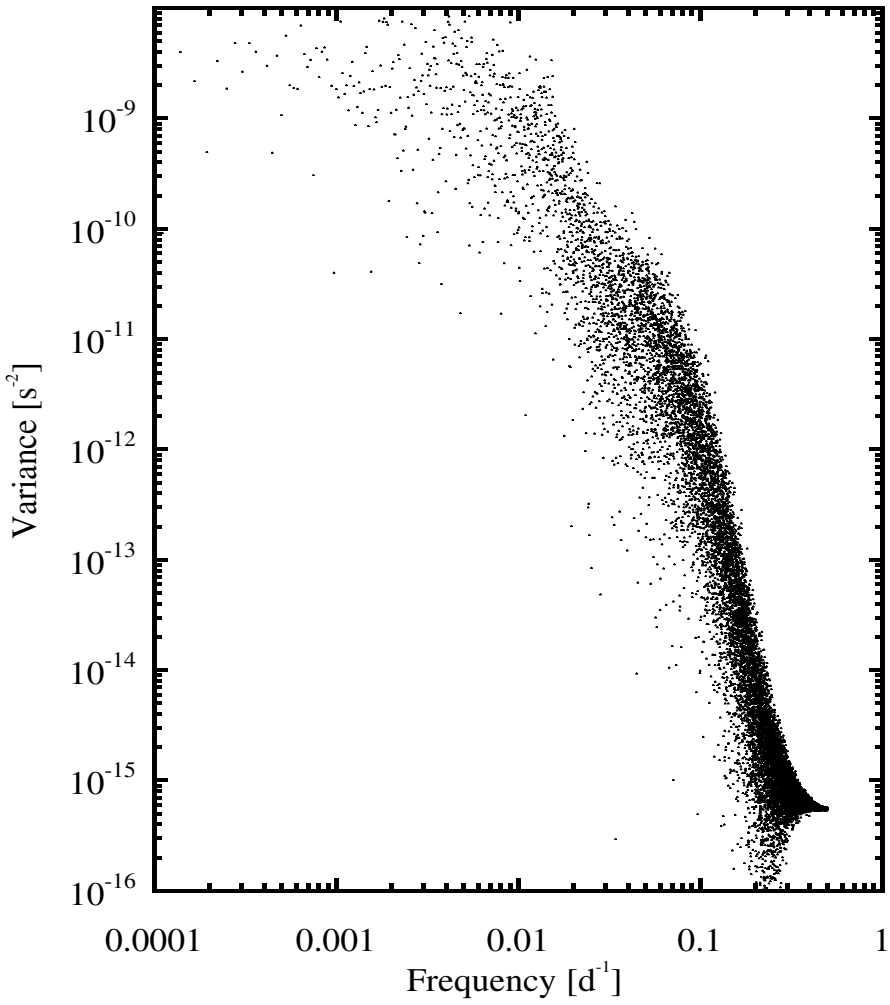

Figure 5: power spectrum of the global mean relative vorticity with $\Delta T_{E-P} =$ 80 K, T21 and $\tau_c = 30$ days. Sampling frequency: 1/day.

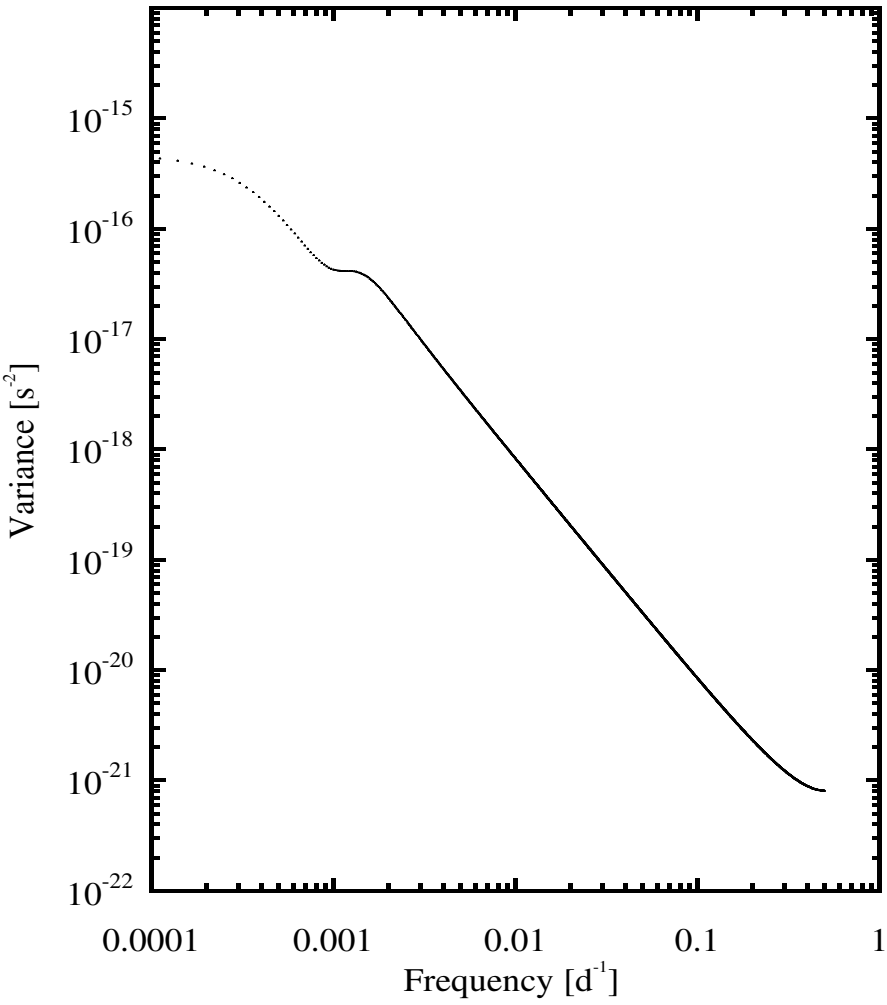

Figure 6: same as Fig. 5 (power spectrum of the global mean relative vorticity), but with $\Delta T_{E-P} = 20$ K.

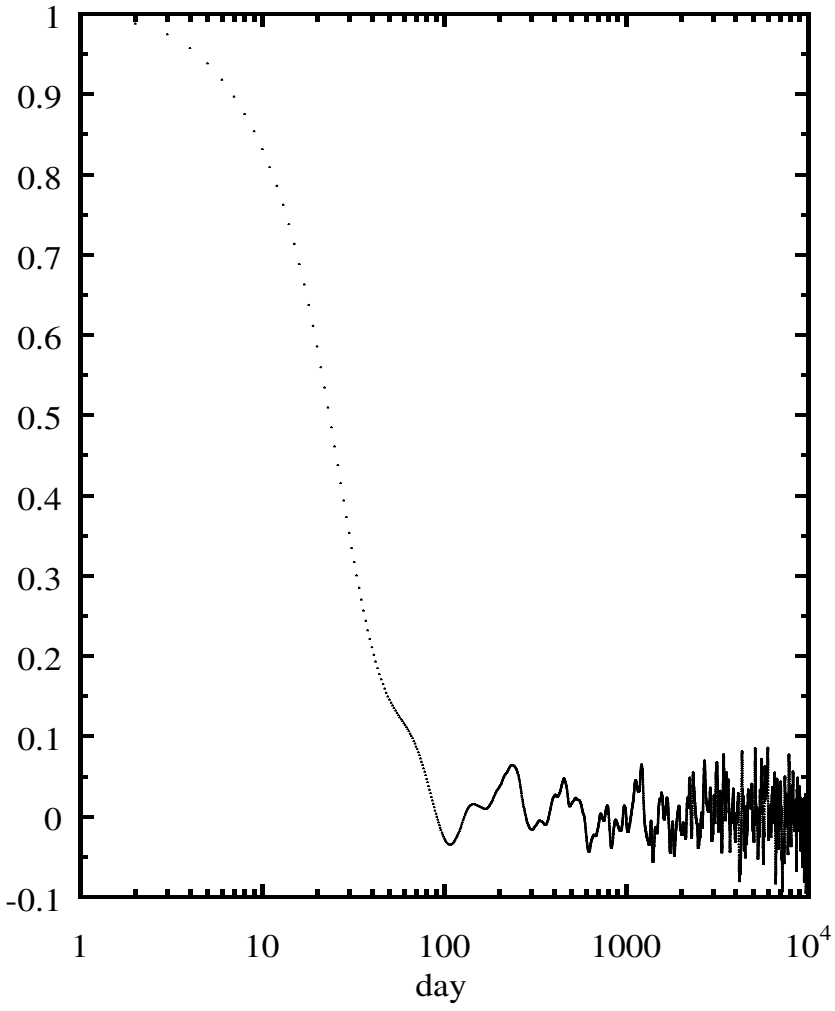

Figure 7: autocorrelation of the global mean relative vorticity with $\Delta T_{E-P} =$ 80 K, T21 and $\tau_c = 30$ days. Sampling frequency: 1/day.

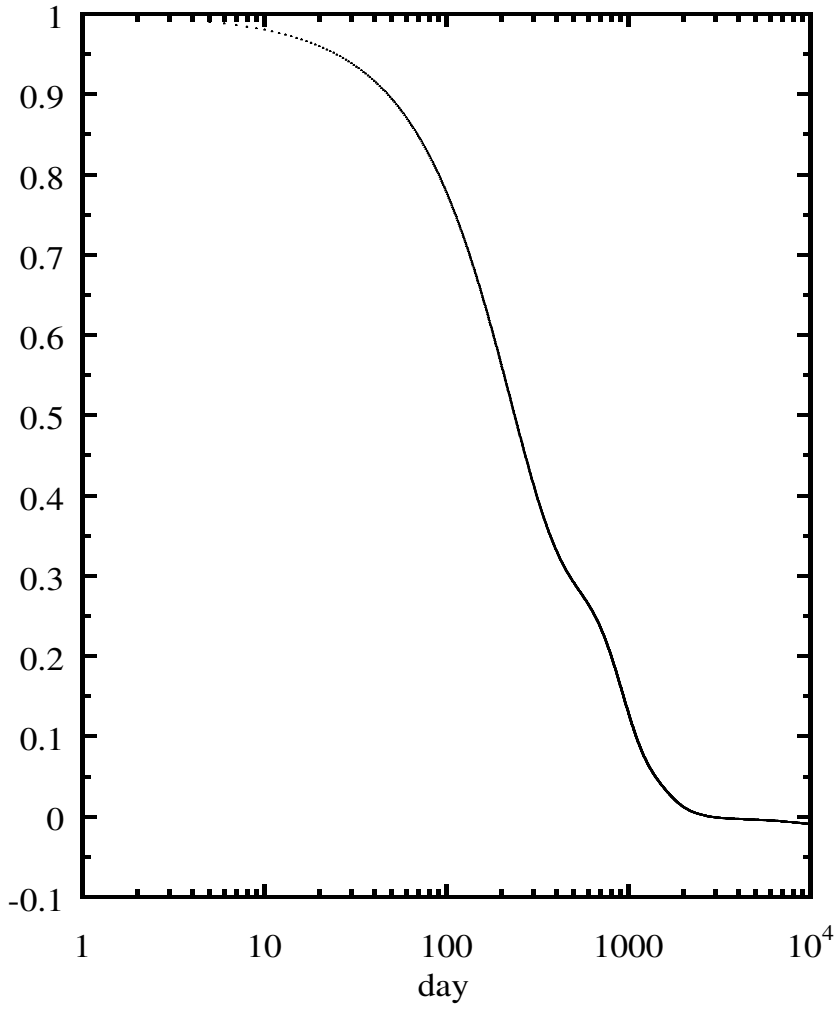

Figure 8: same as Fig. 7 (autocorrelation of the global mean relative vorticity), but with $\Delta T_{E-P} = 20$ K.

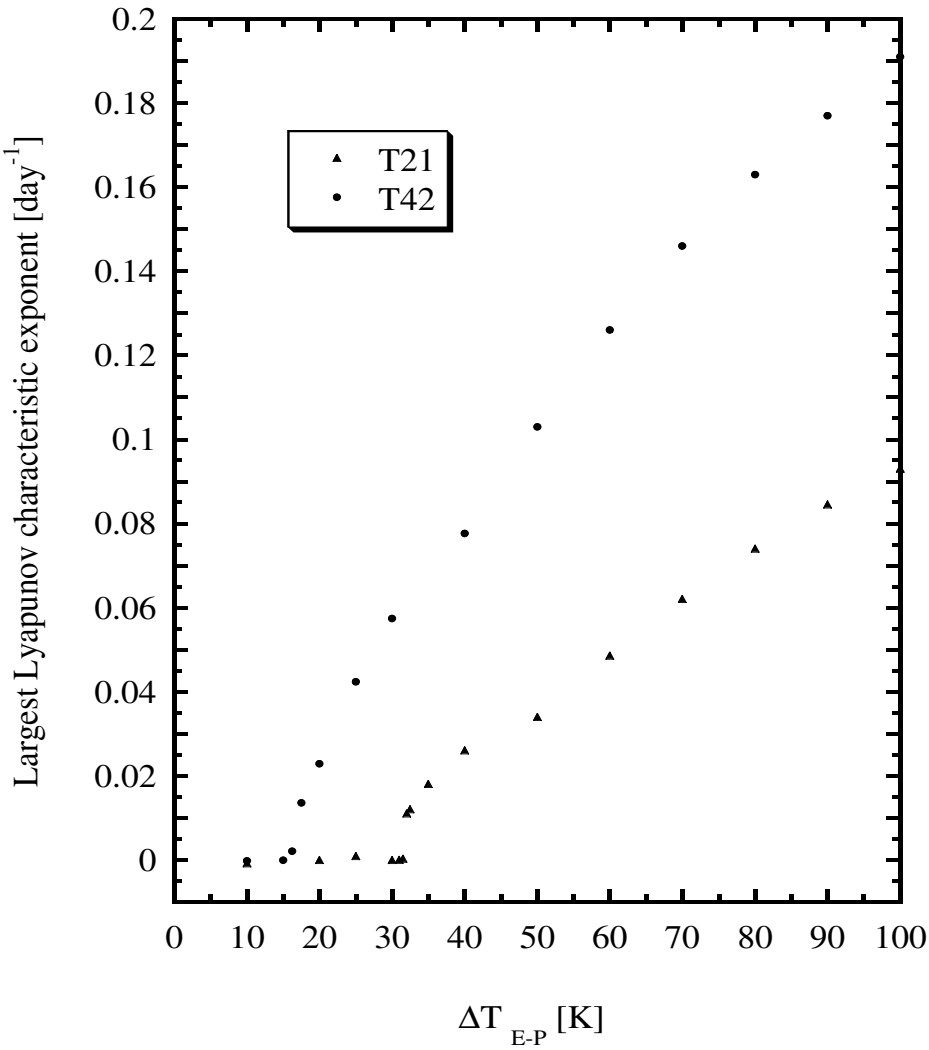

Figure 9: largest LCE vs. ΔT_{E-P} for T21 and T42 horizontal resolutions, with amplitude of initial perturbation $\approx 10^{-2}$ ($\tau_c = 30$ days). The values of the largest LCE for T21 (indicated with triangles) are the same as those reported in Fig. 4.

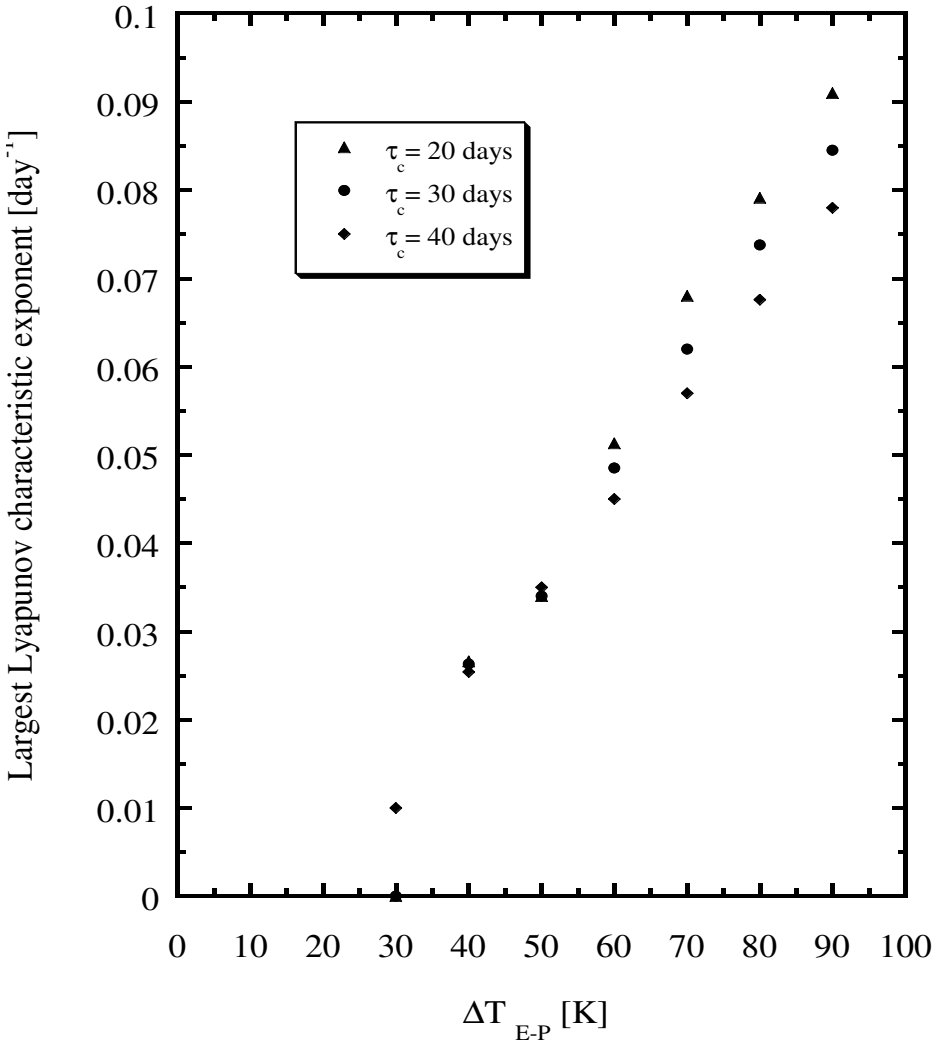

Figure 10: largest LCE vs. ΔT_{E-P} for T21 and different values of τ_c.

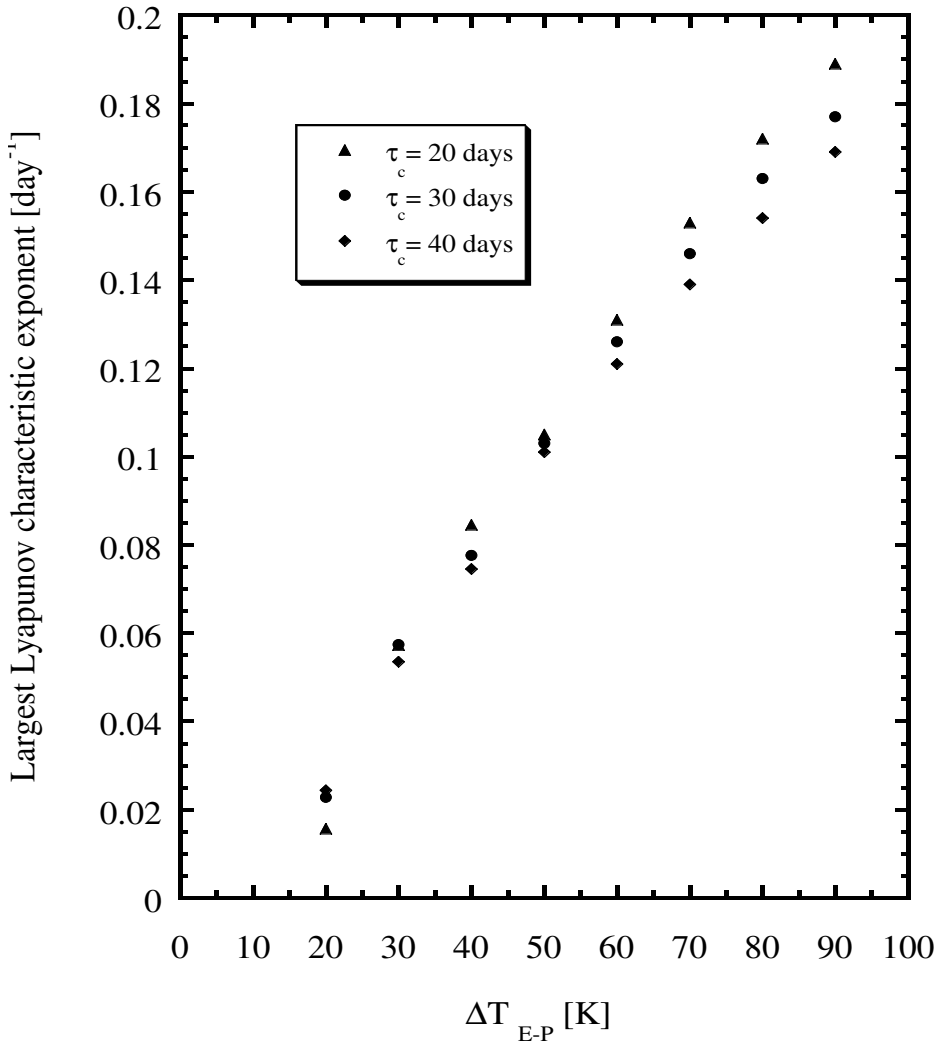

Figure 11: same as Fig. 10 (largest LCE vs. ΔT_{E-P}), but for T42.

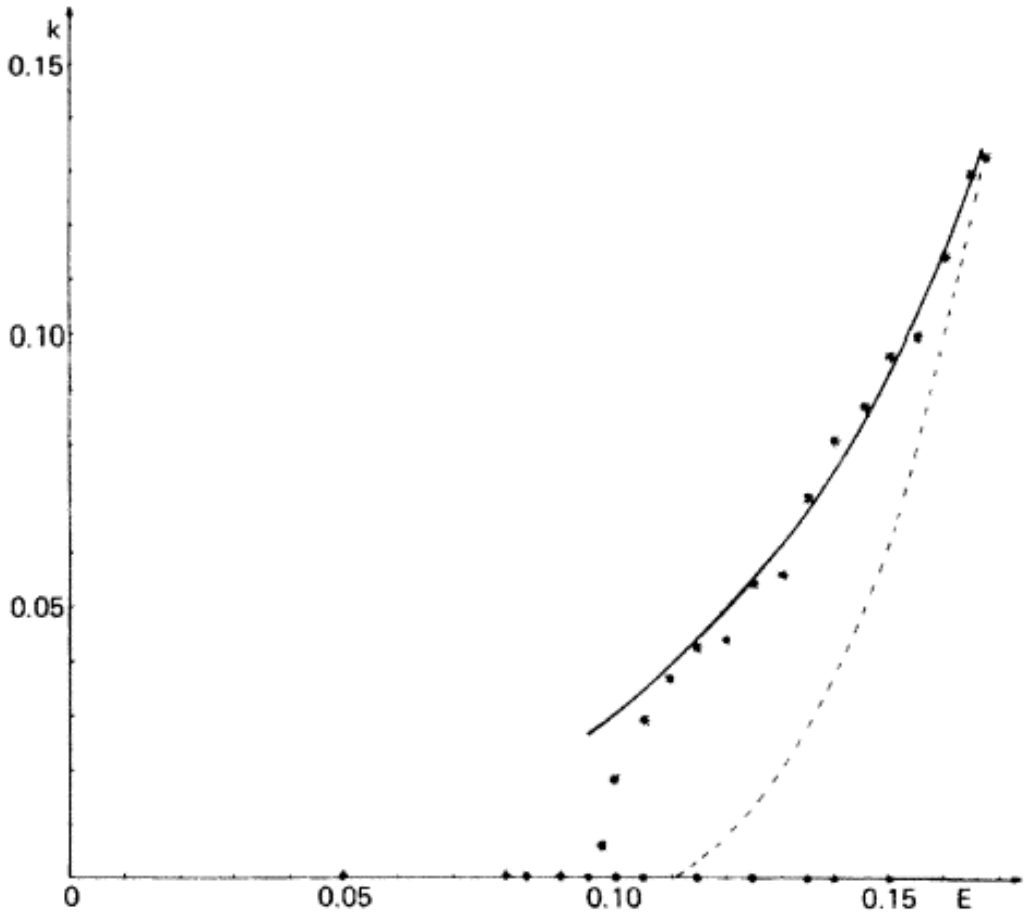

Figure 12: values of the largest LCE, indicated by asterisks, vs. energy E for the Hénon-Heiles model (reprinted with permission from [5], copyright (1976) by the American Physical Society). Vanishing and nonvanishing values of the largest LCE refer to initial conditions taken within the ordered or the stochastic region, respectively (see [5] for further details). To be compared with Figs. (2-4,9).

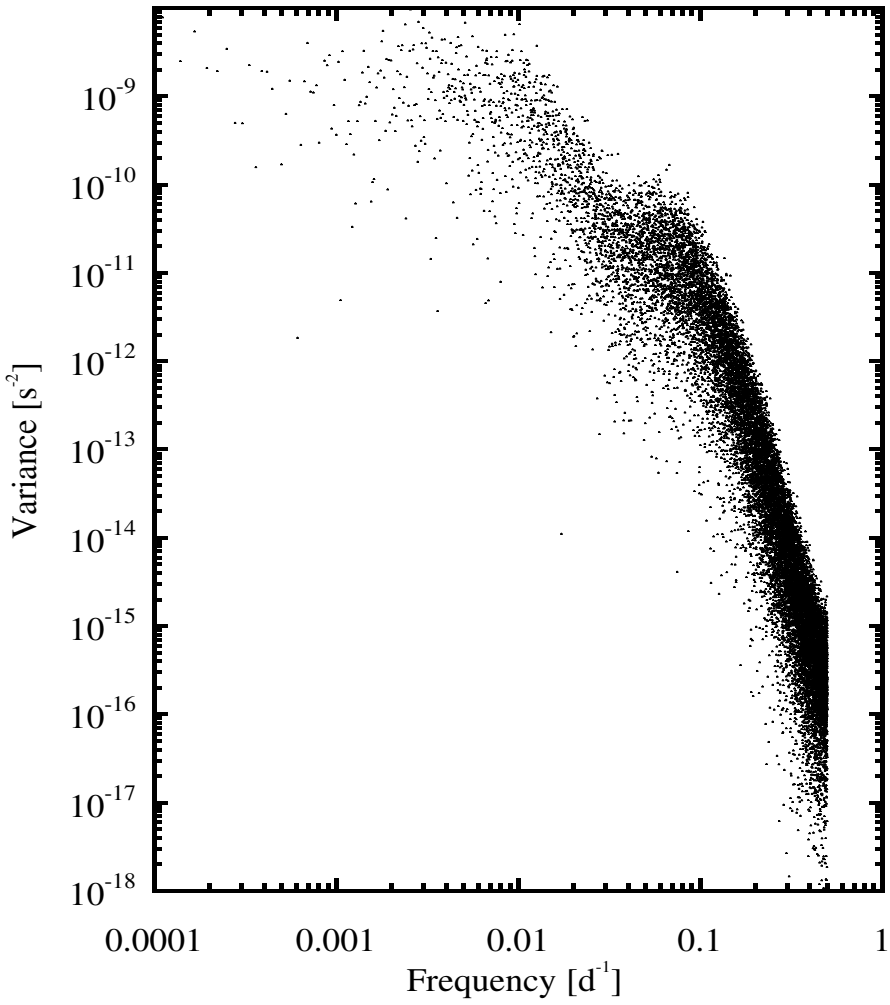

Figure 13: power spectrum of the global mean relative vorticity with $\Delta T_{E-P} = 80$ K, T42 and $\tau_c = 30$ days. Sampling frequency: 1/day.

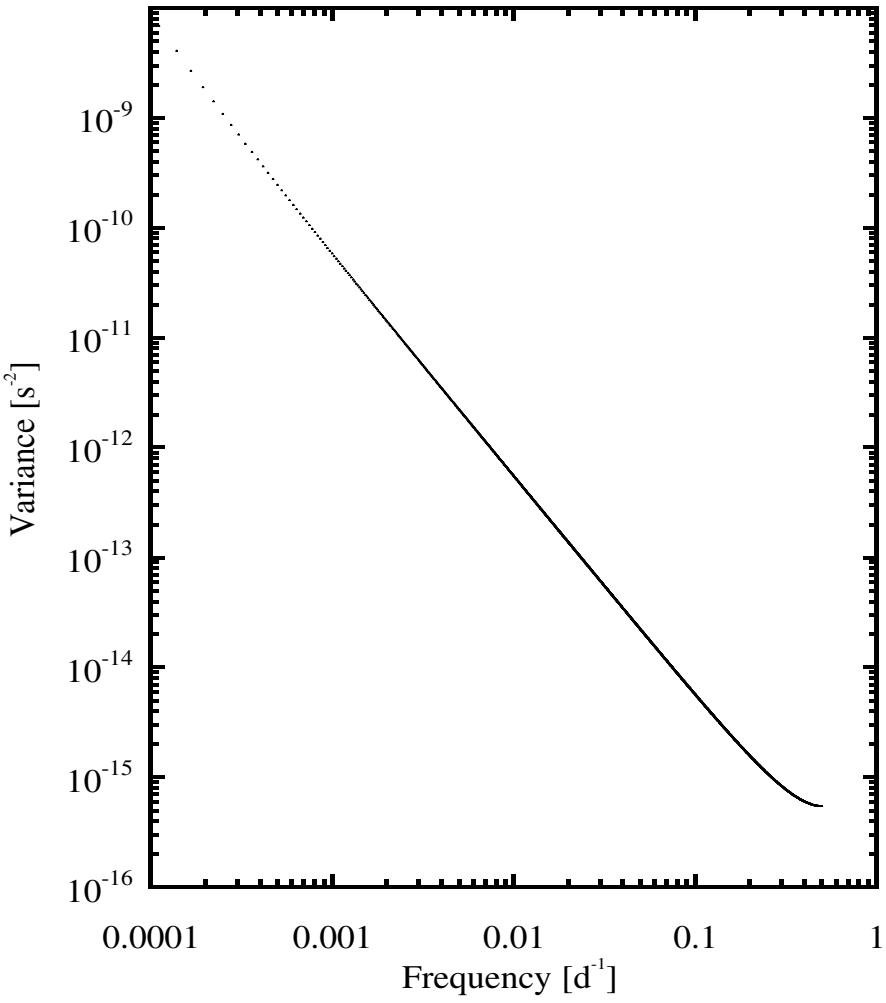

Figure 14: same as Fig.13 (power spectrum of the global mean relative vorticity), but with $\Delta T_{E-P} = 10$ K.

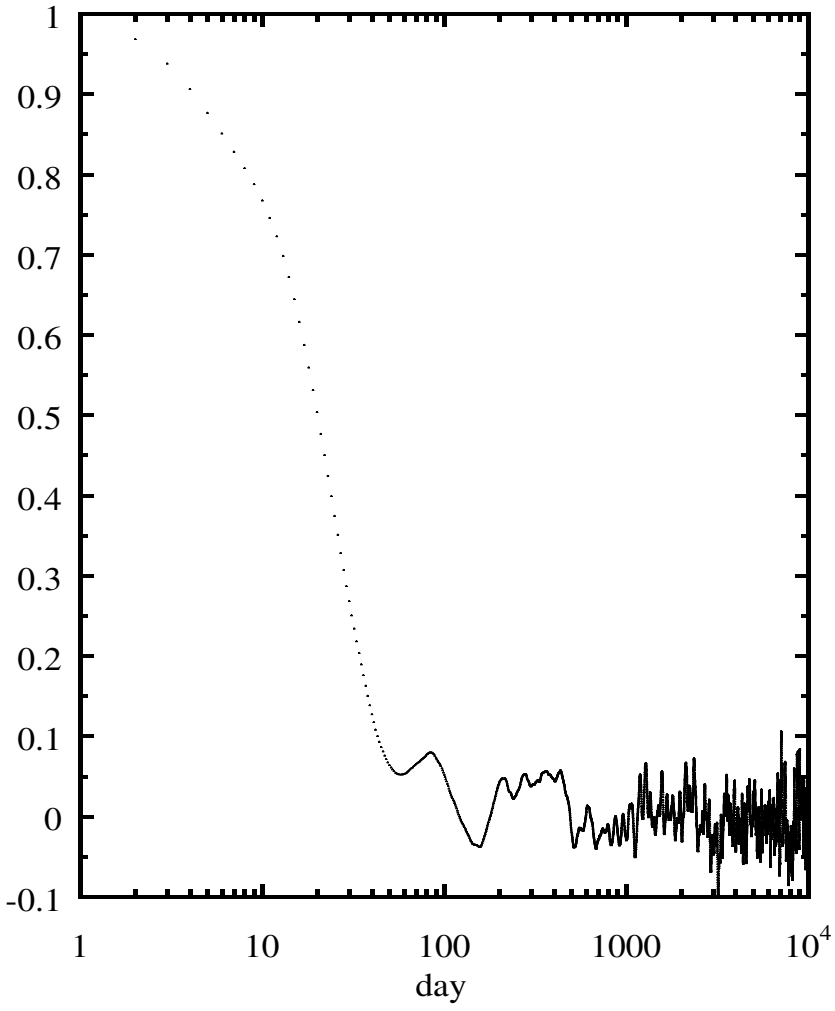

Figure 15: autocorrelation of the global mean relative vorticity with $\Delta T_{E-P} = 80$ K, T42 and $\tau_c = 30$ days. Sampling frequency: 1/day.

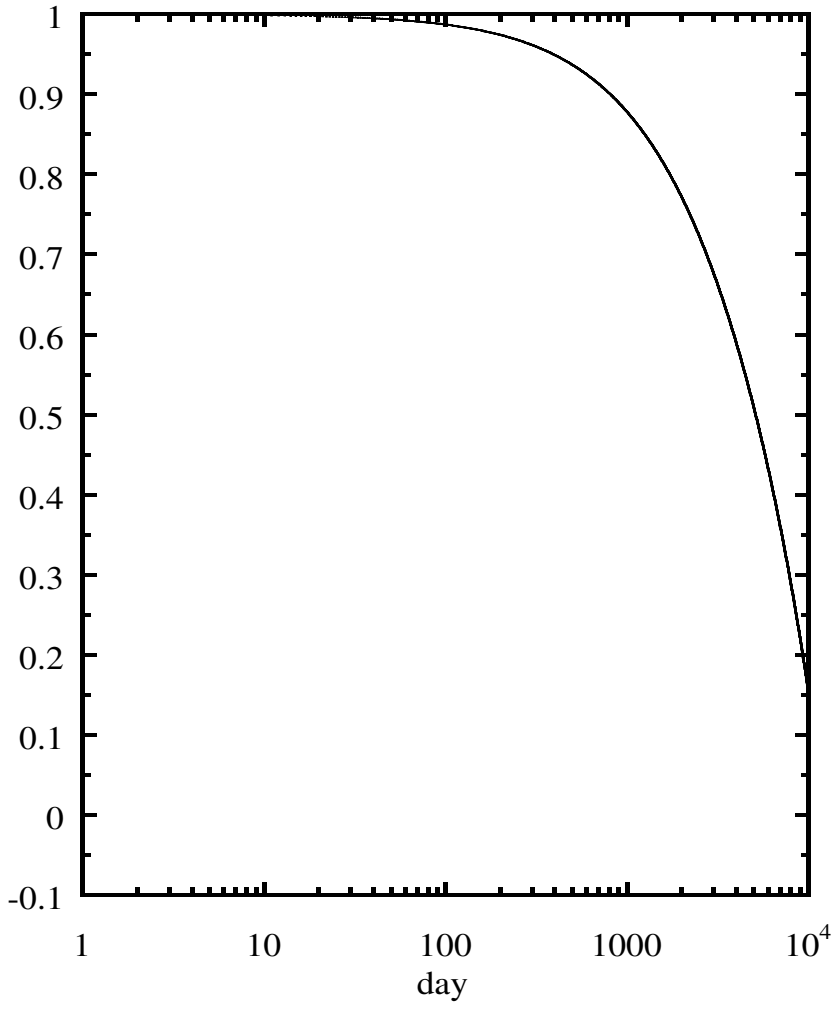

Figure 16: same as Fig. 16 (autocorrelation of the global mean relative vorticity), but with $\Delta T_{E-P} = 10$ K.

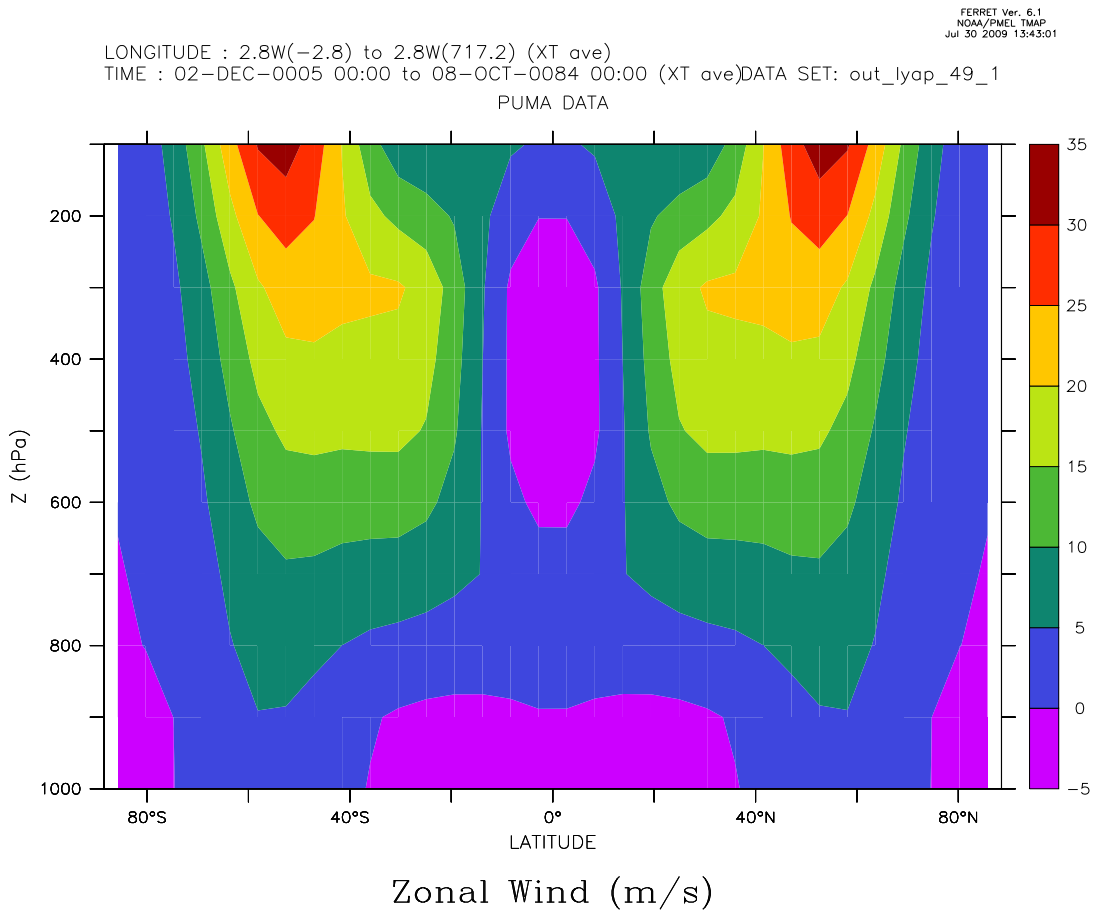

Figure 17: meridional cross section of the time average of the average zonal wind with $\Delta T_{E-P} = 80$ K, T21 and $\tau_c = 30$ days.

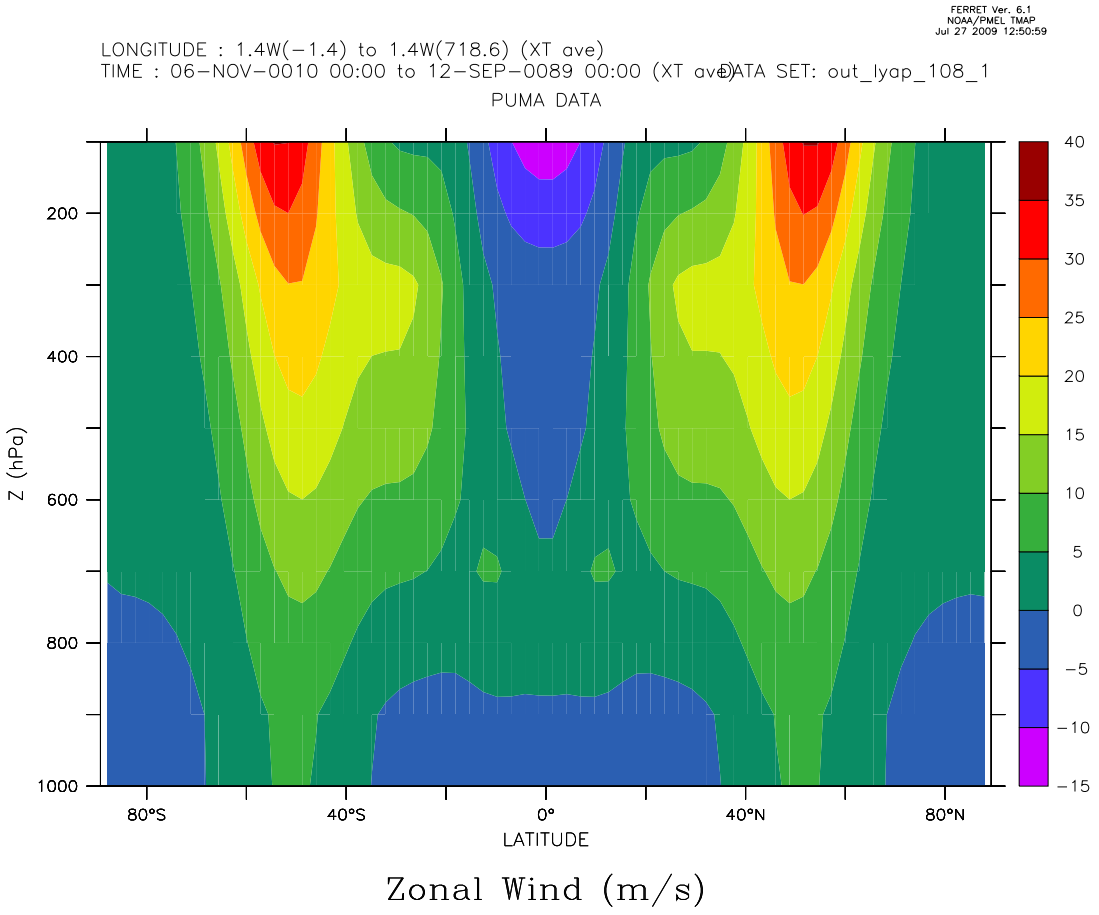

Figure 18: same as Fig. 17 (meridional cross section of the time average of the average zonal wind), but with T42.

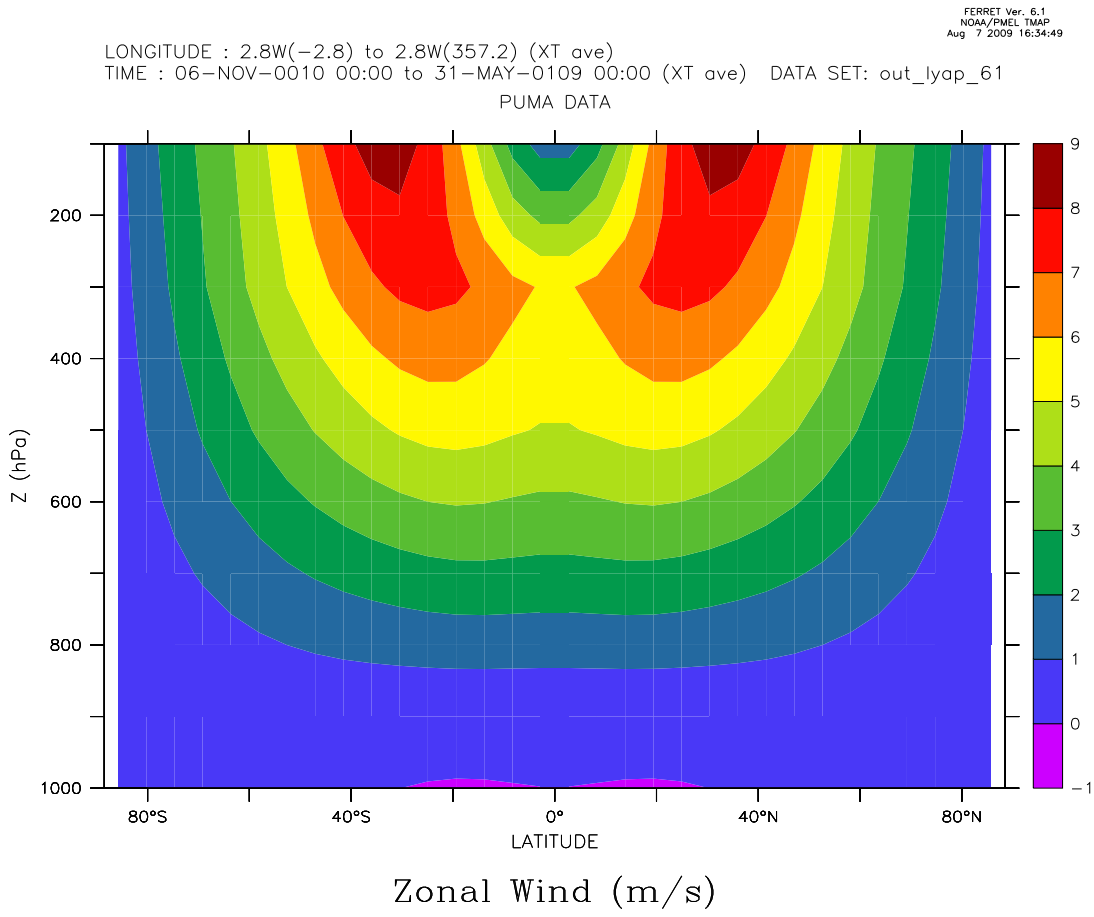

Figure 19: same as Fig. 17 (meridional cross section of the time average of the average zonal wind), but with $\Delta T_{E-P} = 20$ K.

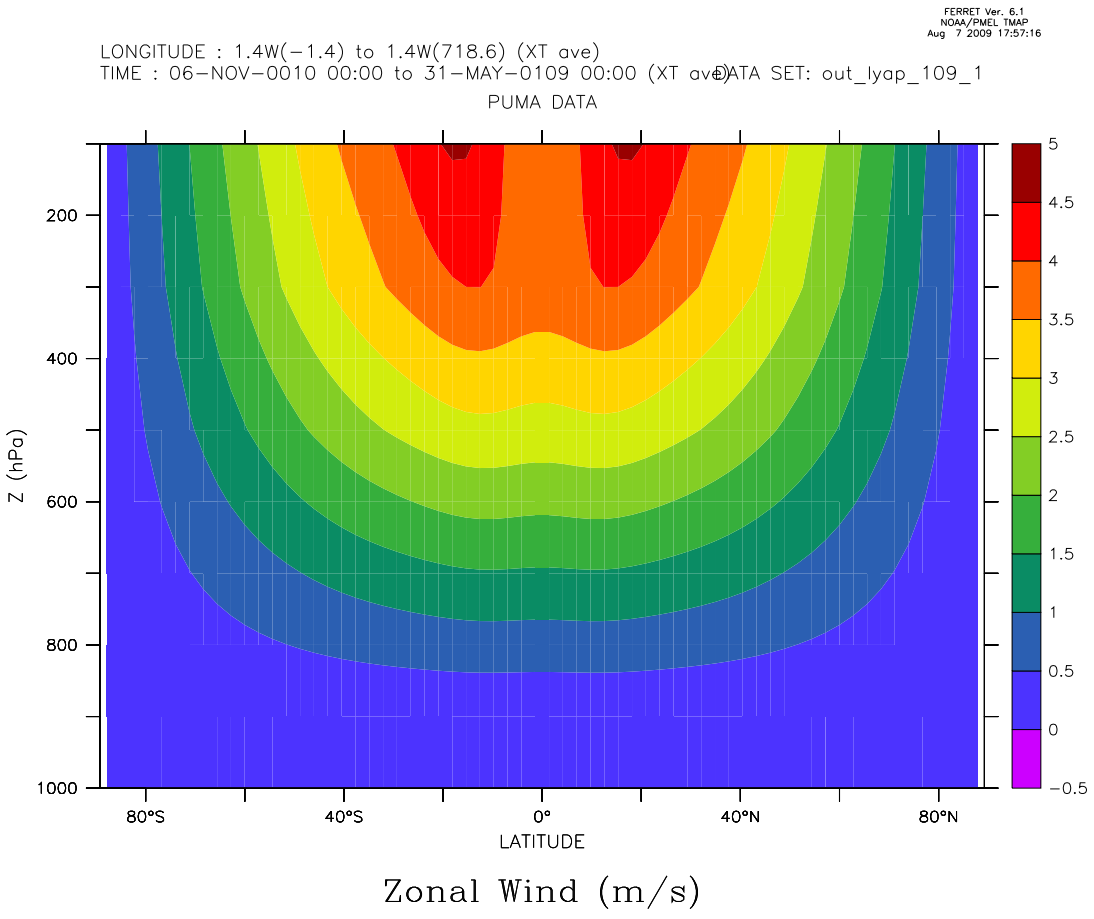

Figure 20: same as Fig. 18 (meridional cross section of the time average of the average zonal wind), but with $\Delta T_{E-P} = 10$ K.

Edito dall' ENEA
Funzione Centrale Relazioni Esterne
Unità Comunicazione
Lungotevere Thaon di Revel, 76 - 00196 Roma
www.enea.it
Stampa: Tecnografico ENEA - CR Frascati
Finito di stampare nel mese di ottobre 2009